

Electronic Supplementary Information

Interlayer electron flow and field shielding in twisted trilayer graphene quantum dots

Xian Wang^a, Yingqi Cui^b, Li Zhang^a and Mingli Yang^{a,*}

a. Institute of Atomic and Molecular Physics, Key Laboratory of High Energy Density Physics of Ministry of Education, Sichuan University, Chengdu 610065, Sichuan University

b. School of Physics and Electronic Engineering, Zhengzhou Normal University, Zhengzhou 450044, China

Contents

Figure S1. Computed averaged γ_{av} (a) and κ (b) for the structures rotating about R_{II} . N is the number of atoms in the QD.

Figure S2. The computed α_{zz} values with the CAM-B3LYP and ω B97XD functionals and the 6-31G(d,p) and 6-31++G(d,p) basis sets.

Figure S3. HOMO and LUMO in RFR with an isovalue of 0.005 a.u. at $\theta = 0^\circ$ (a), 16° (b) and 60° (c), respectively.

Figure S4. PDOS of the top, middle and bottom layers of RFR rotating about the C atom of the innermost shell at $\theta = 0^\circ$ (a), 16° (b) and 60° (c), respectively. The black and blue lines are coincident with each other. The HOMO is marked by dotted line.

Figure S5. The polarizability (α_{zz} , a) and its dipole (α_{zz}^P , b) and CT (α_z^Q , c) parts of the RFR (in blue) and FRR (in red) structures rotating about R_{II} .

Figure S6. The variation in dipole polarizability ($\Delta\alpha_{zz}^P = \alpha_{0,zz} - \alpha_{zz}^P$) of the top (a), middle (b) and bottom (c) layers of the RFR and FRR structures rotating about R_{II} .

Figure S7. Total dq/dF (γ) of the bottom (a), middle (b) and top (c) layers of RFR and RFF structures rotating about R_{II} , respectively.

Figure S8. Atomic γ (in absolute value and in a.u.) in the top, middle and bottom layers of the RFR structure rotating about R_{II} at $\theta = 16^\circ$, respectively.

* Corresponding author. E-mail address: myang@scu.edu.cn (Mingli Yang)

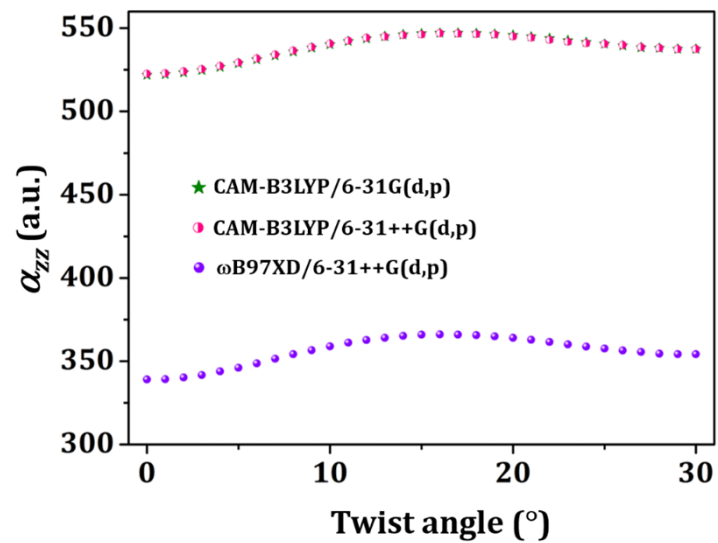


Figure S1. The computed α_{zz} values with the CAM-B3LYP and ω B97XD functionals and the 6-31G(d,p) and 6-31++G(d,p) basis sets.

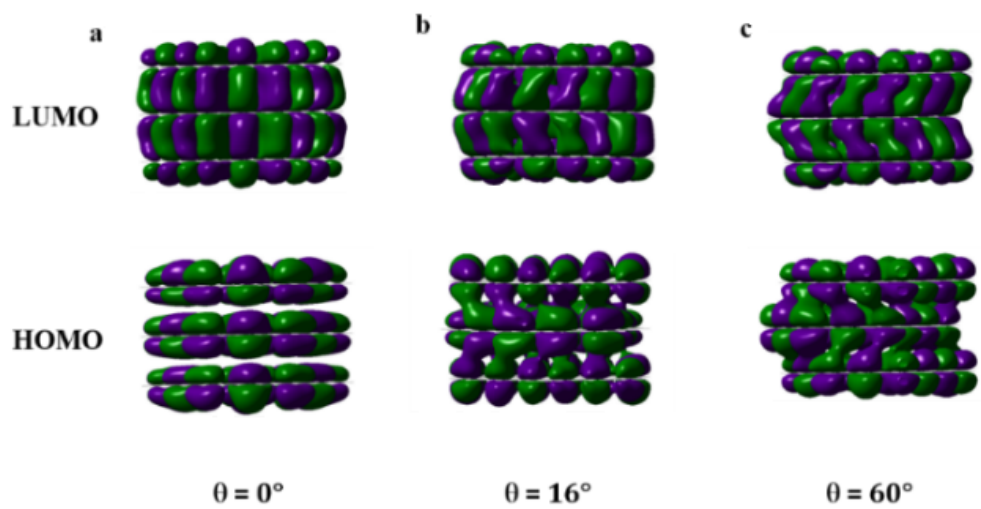


Figure S2. HOMO and LUMO in RFR with an isovalue of 0.005 a.u. at $\theta = 0^\circ$ (a), 16° (b) and 60° (c), respectively.

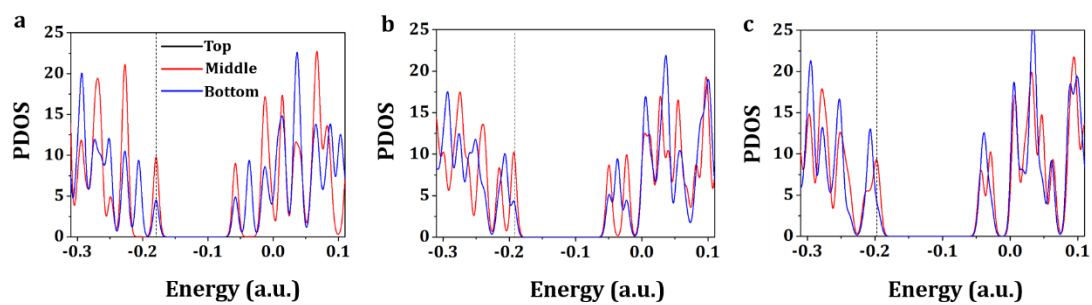


Figure S3. PDOS of the top, middle and bottom layers of RFR rotating about the C atom of the innermost shell at $\theta = 0^\circ$ (a), 16° (b) and 60° (c), respectively. The black and blue lines are coincident with each other. The HOMO is marked by dotted line.

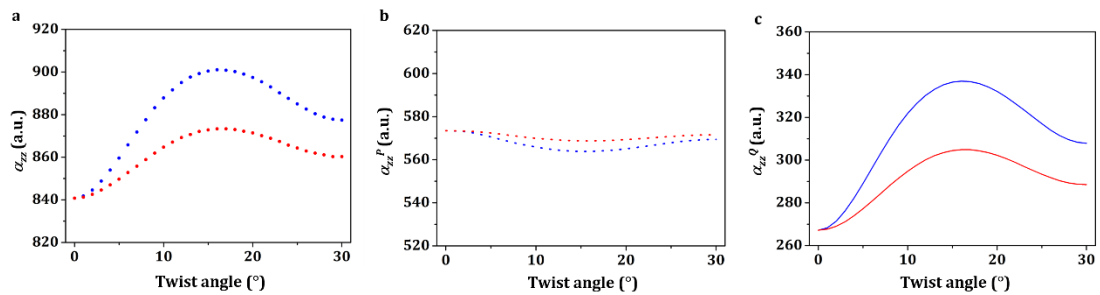


Figure S4. The polarizability (α_{zz} , a) and its dipole (α_{zz}^p , b) and CT (α_{zz}^Q , c) parts of the RFR (in blue) and FRR (in red) structures rotating about R_{II} .

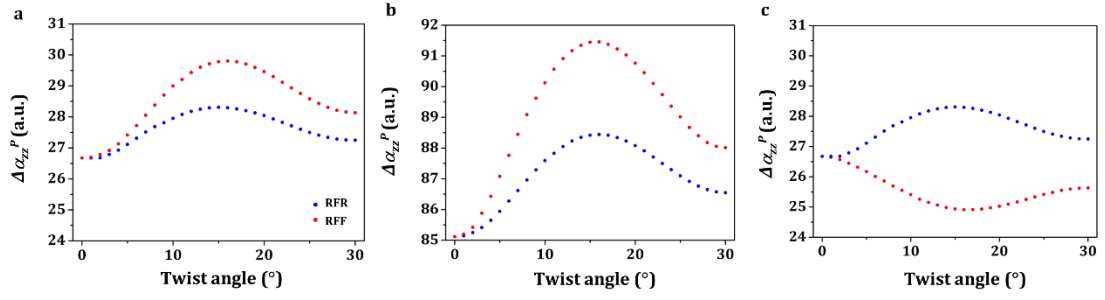


Figure S5. The variation in dipole polarizability ($\Delta\alpha_{zz}^P = \alpha_{0,zz} - \alpha_{zz}^P$) of the top (a), middle (b) and bottom (c) layers of the RFR and RFF structures rotating about R_{II} . $\alpha_{0,zz} = 237.3$ a.u. is the polarizability component of the corresponding monolayer.

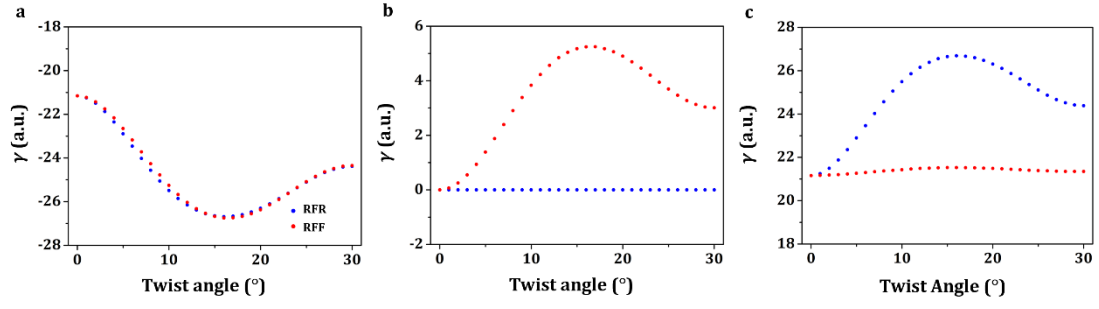


Figure S6. Total dq/dF (γ) of the bottom (a), middle (b) and top (c) layers of RFR and RFF structures rotating about R_{II} , respectively.

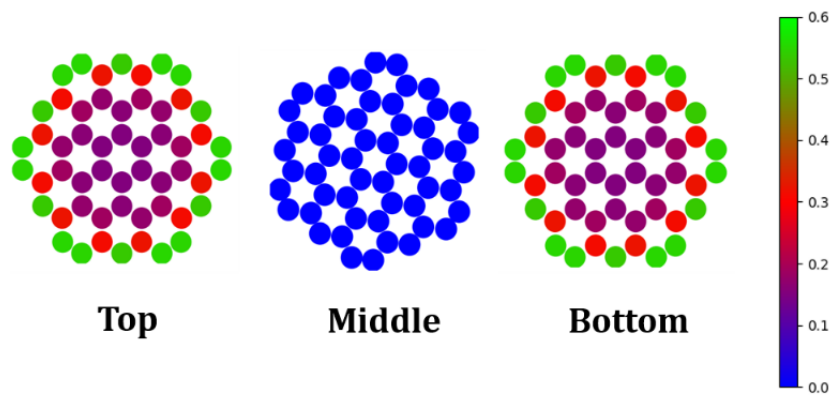


Figure S7. Atomic γ (in absolute value and in a.u.) in the top, middle and bottom layers of the RFR structure rotating about R_{II} at $\theta = 16^\circ$, respectively.

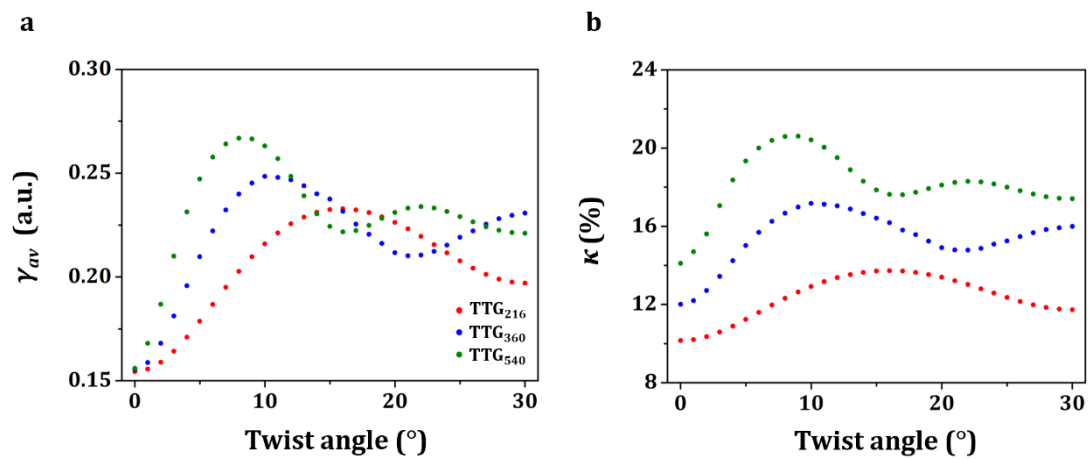


Figure S8. Computed averaged γ_{av} (a) and κ (b) for the structures rotating about R_{II} . N is the number of atoms in the QD.